Ultrasonics - Sonochemistry 64 (2020) 105045

Contents lists available at ScienceDirect

Ultrasonics - Sonochemistry

journal homepage: www.elsevier.com/locate/ultson

Degradation of methylparaben by sonocatalysis using a Co–Fe magnetic carbon xerogel

Athanasios Zanias[a], Zacharias Frontistis[b], John Vakros[a], Olga S. Arvaniti[a], Rui S. Ribeiro[c], Adrián M.T. Silva[c], Joaquim L. Faria[c], Helder T. Gomes[d], Dionissios Mantzavinos[a,*]

[a] Department of Chemical Engineering, University of Patras, Caratheodory 1, University Campus, GR–26504 Patras, Greece
[b] Department of Chemical Engineering, University of Western Macedonia, GR–50100 Kozani, Greece
[c] Laboratory of Separation and Reaction Engineering – Laboratory of Catalysis and Materials (LSRE–LCM), Faculdade de Engenharia, Universidade do Porto, Rua Dr. Roberto Frias, 4200–465 Porto, Portugal
[d] Centro de Investigação de Montanha (CIMO), Instituto Politécnico de Bragança, Campus de Santa Apolónia, 5300–253 Bragança, Portugal

ARTICLE INFO

Keywords:
Advanced oxidation
Sonodegradation
Micropollutants
Cavitation
Low frequency ultrasound
Water quality

ABSTRACT

The degradation of methylparaben (MP) through 20 kHz ultrasound coupled with a bimetallic Co-Fe carbon xerogel (CX/CoFe) was investigated in this work. Experiments were performed at actual power densities of 25 and 52 W/L, catalyst loadings of 12.5 and 25 mg/L, MP concentrations between 1 and 4.2 mg/L and initial pH values between 3 and 10 in ultrapure water (UPW). Matrix effects were studied in bottled water (BW) and secondary treated wastewater (WW), as well as in UPW spiked with bicarbonate, chloride or humic acid. The pseudo–first order kinetics of MP degradation increase with power and catalyst loading and decrease with MP concentration and matrix complexity; moreover, the reaction is also favored at near–neutral conditions and in the presence of dissolved oxygen. The contribution of the catalyst is synergistic to the sonochemical degradation of MP and the extent of synergy is quantified to be > 45%. This effect was ascribed to the ability of CX/CoFe to catalyze the dissociation of hydrogen peroxide, formed through water sonolysis, to hydroxyl radicals. Experiments in UPW spiked with an excess of *tert*-butanol (radical scavenger), sodium dodecyl sulfate or sodium acetate (surfactants) led to substantially decreased rates (i.e. by about 8 times), thus implying that the liquid bulk and the gas-liquid interface are major reaction sites. The stability of CX/CoFe was shown by performing reusability cycles employing magnetic separation of the catalyst after the treatment stage. It was found that the CX/CoFe catalyst can be reused in up to four successive cycles without noteworthy variation of the overall performance of the sonocatalytic process.

1. Introduction

Parabens are esters of p–hydroxybenzoic acid that have been commonly employed as preservatives in food, pharmaceutical and cosmetic industries. They are inexpensive agents with considerable antimicrobial activity, high water solubility and high stability in a wide pH range [1]. However, their use has recently raised concerns since there are studies reporting that parabens may be related to human breast cancer, as well as to behave as endocrine disruptors [2,3], which led to the replacement of parabens from various products.

Although the occurrence of parabens is limited to < 0.8% in cosmetics, < 1% in pharmaceuticals and < 0.1% in foodstuff [4], they have been consistently detected in various environmental matrices [5]. This occurs due to industrial wastewater discharges and to the low efficiency of the conventional urban wastewater treatment plants based on traditional biological treatments, to remove biorecalcitrant and persistent organic pollutants, typically found in trace amounts (in the range of ng/ L to μg/L), such as parabens [5]. In this respect, recent research efforts have been focused on the study of various advanced oxidation processes (AOPs) as effective treatment technologies for parabens degradation, including photocatalysis [6–9], activation of persulfate [10,11], electrochemical processes [12] and ultrasound irradiation [13,14]. The latter relies on the propagation of ultrasonic waves through a liquid, which alters the local pressure with time and space and results in the formation of bubbles. The radius of the bubble will expand, contract and/or collapse in response to these pressure changes. This phenomenon is called transient cavitation and is characterized by high temperatures and pressures inside the bubble. During

* Corresponding author.
E-mail address: mantzavinos@chemeng.upatras.gr (D. Mantzavinos).

https://doi.org/10.1016/j.ultsonch.2020.105045
Received 13 September 2019; Received in revised form 21 January 2020; Accepted 24 February 2020
Available online 25 February 2020

the final stage of collapse, the velocity of the liquid gas interface approaches the speed of sound in the liquid and the localized temperature can rise up to 3000 °C. Such temperatures are responsible for water decomposition and the subsequent production of H˙ and HO˙ radicals [15]. The latter can oxidize organic pollutants in the liquid bulk and/or in the vicinity of the bubble, while pyrolytic degradation in the gas–liquid interface and/or inside the bubble may also occur depending on the physicochemical properties of the pollutants and the specific reaction conditions.

The effect of medium to high ultrasound frequency (i.e. 200–1000 kHz) on methylparaben (MP) degradation was studied by Sasi et al [13] reporting on the effect of various operating conditions on performance, such as power, pH, MP concentration, water matrix constituents and co–treatment with other pollutants. In addition to the operating conditions (namely ultrasound frequency in the range 572–1164 kHz), Savun-Hekimoğlu and Ince studied the effect of bubbling gas (air, argon and ozone) on the oxidation of MP [16]. Our group investigated [14] the low frequency (i.e. 20 kHz) sonochemical degradation of ethylparaben with respect to the most statistically significant operating conditions. Amongst others, it was found that the simultaneous use of persulfate salt enhanced degradation since ultrasound may activate persulfate to generate sulfate radicals. Another way to influence the performance is associated with the use of a solid material that may act as a nucleus facilitating cavitation and/or a catalyst, enhancing radicals formation in a process typically called sonocatalysis [16,17].

In this perspective, this study deals with the 20 kHz sonochemical degradation of MP in the presence of a magnetic carbon xerogel containing cobalt and iron (CX/CoFe). Such xerogels containing either of the two metals or both were synthesized previously and tested successfully for the degradation of sulfamethoxazole [18] and 4-nitrophenol [19] by catalytic wet peroxide oxidation, and bisphenol A [20] and propylparaben [21] by activated persulfate. By selecting a heterogeneous catalyst that has already been thoroughly studied and shown to perform well in two different environmental catalytic applications, it was possible to focus on exploring the interface between materials science and sonochemistry. As a consequence, this study reports for the first time the beneficial integration of carbon xerogels with ultrasound for the synergistic degradation of parabens. This enhanced degradation is a step forward towards developing effective technologies for the degradation of parabens. In addition, it provides the mechanistic pathways for the occurrence of several species endogenous to sonochemical processes, as well as it studies (i) the effect of various operating parameters on reaction kinetics, (ii) the addition of persulfate salt as an extra source of radicals, (iii) matrix effects (in bottled water, secondary treated wastewater, and ultrapure water spiked with bicarbonate, chloride and humic acid), and (iv) catalyst stability in a series of four runs performed with consecutive reuse of CX/CoFe.

2. Materials and methods

2.1. Preparation and characterization of CX/CoFe

Details of the CX/CoFe catalyst synthesis and characterization procedures and techniques can be found elsewhere [18]. In brief, the carbon xerogel consists of interconnected carbon microspheres with iron and cobalt microparticles embedded in its structure. This can be done through a simple preparation route in which occurs the inclusion of iron (considering a Fe/resorcinol molar ratio of 0.05) and cobalt (considering a Fe/Co molar ratio of 2) precursors during the sol–gel polymerization of resorcinol with formaldehyde, followed by thermal annealing. The amount of iron incorporated during the synthesis was selected based on the typical metal content of carbon-supported iron catalysts for environmental catalytic applications (in the range of 4 to 7 wt%) [22]; while the amount of cobalt was selected considering the optimum value previously reported for carbon-supported iron-copper catalysts [23]. The resulting powder CX/CoFe catalyst has a specific surface area of 530 m^2/g and contains 4.6 wt% iron and 2.1 wt% cobalt [18].

2.2. Experimental procedures and analytical protocols

Sonochemical experiments were carried out using a Branson 450 ultrasonic generator operating at a fixed frequency of 20 kHz and a maximum nominal power of 450 W and connected to a horn–type transducer made of titanium with a tip diameter of 1 cm. The experiments were performed in a cylindrical and double–walled pyrex vessel, which was open to the atmosphere (unless otherwise stated). The working volume was 0.2 L and the bulk temperature was kept constant at 20 °C with a temperature control unit. Ultrasound irradiation was emitted in the liquid phase through the horn tip, which was positioned in the middle of the vessel at a distance of 3 cm from the bottom; calorimetry was employed to measure the actual power entering the liquid. Sonocatalytic experiments started upon adding the CX/CoFe catalyst and immediately turning on the ultrasonic generator, that time being considered as $t_0 = 0$ min. Silent adsorption runs were performed in the absence of ultrasonic irradiation, while sonochemical degradation was also performed in the absence of CX/CoFe. Additional experiments were performed with added sodium persulfate (SPS), in the presence of conventional radical scavengers and surfactants, and by purging oxygen from the reaction mixture.

Samples of 1.2 mL were withdrawn periodically from the reactor, filtered with 0.22–μm PVDF filters and analyzed using high pressure liquid chromatography (Waters Alliance 2695) to monitor MP concentration. Separation was achieved on a Kinetex C18 2.6 μm 150 × 2.1 mm column (Phenomenex, USA) thermostatted at 45 °C. The mobile phase consisting of 68:32 water:acetonitrile eluted isocratically, while the injection volume was 40 μL. Detection was achieved through a photodiode array detector (Waters 2996 PDA) set at 254 nm.

The concentration of H_2O_2 formed during the process was determined photometrically at 450 nm. The determination based on the reaction of H_2O_2 with ammonium metavanadate in acidic medium, which results in the formation of a red–orange color peroxovanadium cation [24].

2.3. Chemicals

Methylparaben (MP) analytical grade, sodium persulfate (SPS, 99+ %), acetonitrile (99.9%), humic acid (HA, technical grade), sodium hydroxide (98 wt%), and sulfuric acid (95 wt%) were obtained from Sigma Aldrich, while *t*-butanol (99%), glucose (99%), sodium dodecyl sulfate (SDS) and sodium acetate (99%) were purchased from Fluka.

The water matrices used were: (i) ultrapure water – UPW (pH = 6.5, 0.056 μS/cm conductivity), (ii) drinking water (pH = 7.8, 357 μS/cm conductivity, 250 mg/L HCO_3^-, 9.1 mg/L SO_4^{2-}, 5 mg/L Cl^-) obtained from commercially available bottled water – BW; (iii) secondary treated wastewater – WW (pH = 7.9, 6.2 mg/L total organic carbon, 1.07 mg/L total suspended solids, 18.9 mg/L chemical oxygen demand, 311 μS/cm conductivity, 30 mg/L SO_4^{2-}, 0.44 mg/L Cl^-) collected from the wastewater treatment plant of the University of Patras campus, Greece.

3. Results and discussion

Fig. 1 shows concentration–time profiles for MP degradation during ultrasound irradiation at 25 and 52 W/L actual power density, as well as for the integration of the CX/CoFe catalyst (25 mg/L) with ultrasound, and for MP silent removal due to adsorption on CX/CoFe. The latter is responsible for 29.2% removal after 60 min of adsorption on 25 mg/L catalyst. Ultrasound in the absence of catalyst results in 10% MP degradation after 60 min of irradiation at 25 W/L and this increases to 64% at 52 W/L (the experiment at 25 W/L was extended to 120 min

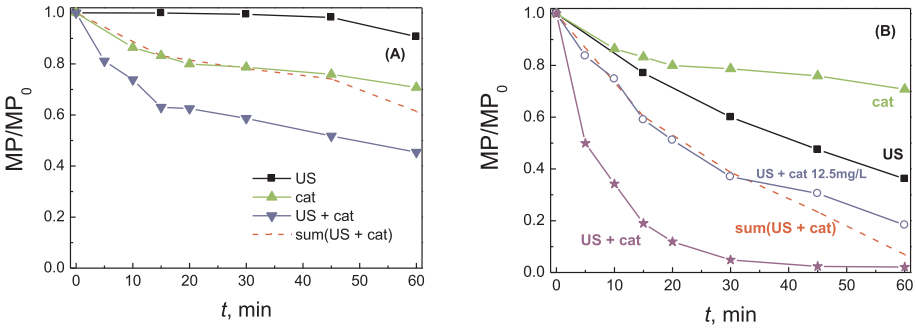

Fig. 1. Synergy between US and 25 mg/L CX/CoFe for the sonocatalytic degradation of 1 mg/L MP in UPW. (A) 25 W/L; (B) 52 W/L. An additional sonocatalytic experiment with 12.5 mg/L CX/CoFe is given in (B) and shown by empty circles.

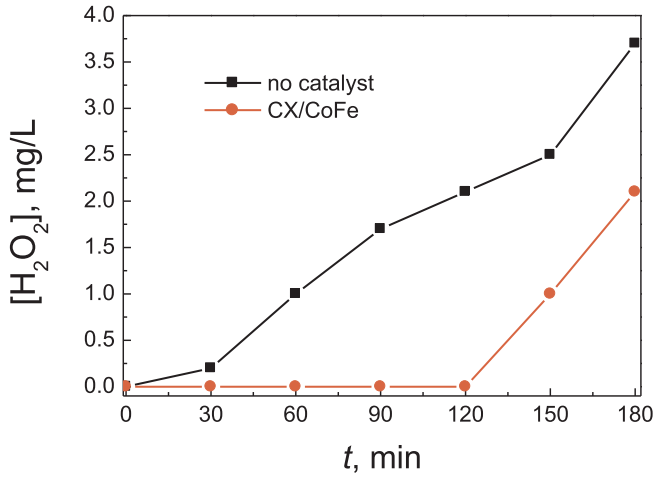

Fig. 2. Formation of H_2O_2 during water sonolysis at 52 W/L with and without CX/CoFe (25 mg/L).

(not shown for uniformity of presentation) leading to 37.3% degradation). Enhanced cavitational activity occurring at increased levels of ultrasound power presumably results in increased degradation rates [15].

The sonocatalytic experiment results in 54.6% MP degradation after 60 min at 25 W/L and almost complete degradation within 45–60 min at 52 W/L. The dashed lines shown in Fig. 1 correspond to the computed concentration profiles of MP degradation if the respective data from the individual processes, i.e. sonochemical degradation and silent adsorption, were simply added up together. It is evident that the effect of coupling ultrasound irradiation with the catalyst is synergistic rather than cumulative since the actual profiles of the sonocatalytic process lie below the computed profiles. To quantify the extent of synergy (S), one can employ the following formula [25]:

$$S(\%) = 100\frac{k_{US+cat} - k_{US} - k_{cat}}{k_{US+cat}} \quad (1)$$

where k_{US+cat}, k_{US} and k_{cat} refer to the apparent rate constants of the sonocatalytic, sonochemical and adsorption processes, respectively.

On the assumption that the aforementioned processes can be described by a pseudo–first order kinetic expression, in terms of MP concentration ([MP]):

$$-\frac{d[MP]}{dt} = k[MP] \quad (2)$$

k values can be computed from the data of Fig. 1. Following this methodology, the extent of synergy is equal to 46% and 74% for the runs at 25 and 52 W/L. According to Eq. (1), positive S values indicate process synergy, negative values are characteristic of an inhibitory effect, while a zero value is typical of a cumulative (additive) effect. Synergy can be explained on the grounds that catalyst particles act as nuclei for the formation of more cavitation bubbles, whose collapse results in more hydroxyl radicals and other reactive species in the liquid. This is consistent with the fact that MP degradation rate decreases with decreasing catalyst concentration, as can be seen in Fig. 1B, from 0.079 min^{-1} at 25 mg/L to 0.029 min^{-1} at 12.5 mg/L. Moreover, particles are better dispersed in the liquid due to the action of ultrasound, while mass transfer from the liquid to the particle surface may also be enhanced.

Furthermore, CX/CoFe may catalyze the decomposition of H_2O_2 formed during ultrasound irradiation, thus mimicking a Fenton–like reaction. Specifically, hydroxyl radicals, formed via water sonolysis (Eq. (3)) can partly recombine yielding hydrogen peroxide (Eq. (4)), which in turn reacts with hydrogen to regenerate hydroxyl radicals (Eq. (5)) [26,27]. In addition, iron in the catalyst spinel can react with H_2O_2 (Eq. (6)) to facilitate the regeneration of hydroxyl radicals.

$$H_2O \overset{)))}{\rightarrow} H\cdot + HO\cdot \quad (3)$$

$$HO^{\cdot} + HO^{\cdot} \rightarrow H_2O_2 \quad (4)$$

$$H_2O_2 + H^{\cdot} \rightarrow H_2O + HO^{\cdot} \quad (5)$$

$$Fe^{2+} + H_2O_2 \rightarrow Fe^{3+} + HO^{\cdot} + OH^{-} \quad (6)$$

The formation of H_2O_2 during water sonolysis was evidenced experimentally, as can be seen in Fig. 2. In the absence of catalyst, H_2O_2 concentration increases steadily over time reaching ca. 4 mg/L after 180 min of sonication. Nonetheless, its concentration is suppressed considerably in the presence of catalyst presumably due to the occurrence of reaction (6). Indeed, the ability of CX/CoFe to act as heterogeneous Fenton catalyst was already shown under different operating conditions [18,19]. Moreover, interactions between the generated radicals and the solid surface cannot be excluded and this would also restrict the occurrence of reaction (4).

Fig. 3 shows the detrimental effect of increasing MP concentration on its degradation; a 6.5–fold rate decrease occurs when MP concentration increases from 1 to 2–4.2 mg/L. This implies that the reaction is not truly first order since the rate constant changes with changing MP concentration and this is associated with the substrate to oxidizing species relative concentration. At a fixed set of operating conditions (i.e. ultrasound frequency and power density, catalyst concentration, etc.), the oxidants are produced at a certain rate and, therefore, their concentration is expected to be nearly constant. In this sense, the critical factor is the substrate concentration which will dictate whether oxidants are the limiting reactant or not and, consequently, the degradation kinetics.

In further experiments, the effect of adding sodium persulfate on process performance was investigated and the results are shown in Fig. 4. The rational for this set of experiments has to do with the fact that SPS activation to generate extra sulfate and hydroxyl radicals can

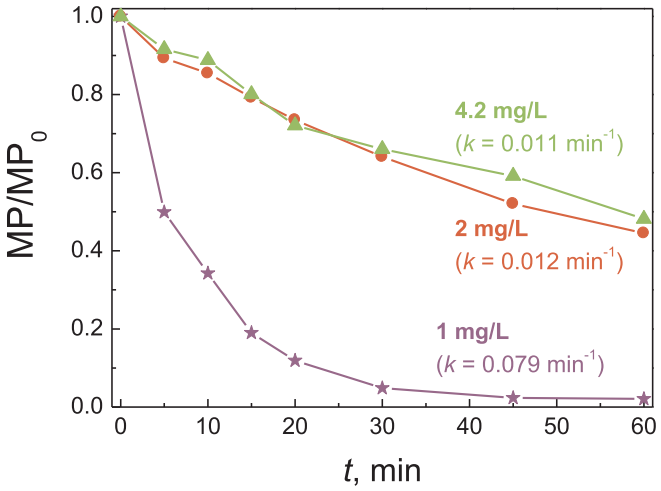

Fig. 3. Effect of initial MP concentration on its sonocatalytic degradation at 52 W/L with 25 mg/L CX/CoFe in UPW. Numbers in brackets show *k* values in min^{-1}.

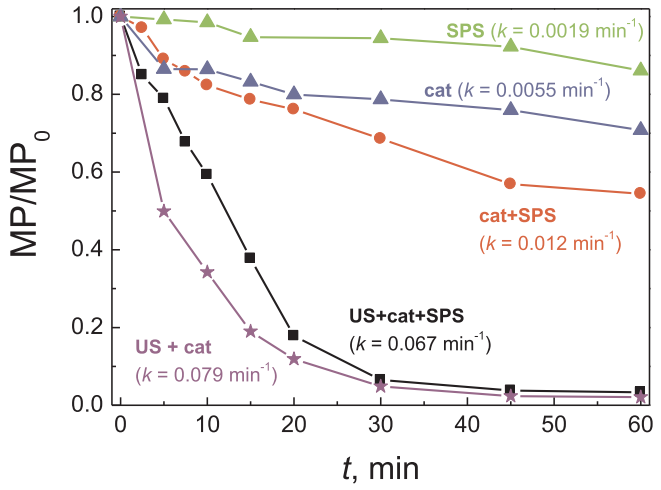

Fig. 4. Effect of 250 mg/L SPS addition on 1 mg/L MP sonocatalytic degradation at 52 W/L with 25 mg/L CX/CoFe in UPW. The respective silent runs are also shown. Numbers in brackets show *k* values in min^{-1}.

be implemented by both the carbocatalyst containing iron and cobalt [28–31] and the action of ultrasound [32]. Indeed, the catalyst seems to activate SPS, thus enhancing MP removal during the silent run; this is consistent with previous findings of our group concerning the removal of bisphenol A by the CX/CoFe–SPS system [20]. Nonetheless, the combined action of catalyst and ultrasound to activate SPS is detrimental to MP degradation in comparison to the sonocatalytic process. Applying by analogy Eq. (1), the extent of synergy is negative (−35.8%), clearly indicating an antagonistic effect.

All the experiments described so far were performed in UPW, thus ignoring the likely interactions amongst the target pollutant, the catalyst, the oxidants and the water matrix, and the non–target constituents. Fig. 5a shows the detrimental effect of actual water matrix (WW and BW) on MP degradation; the rate in UPW decreases by about 40% in BW and 80% in WW. Inorganic constituents in actual matrices include various anions and cations (see also Section 2.3), while natural organic matter can also be found; the latter is usually represented by humic (HA) and fulvic acids. Fig. 5a also shows an experiment with UPW spiked with 10 mg/L HA to simulate the organic content of the WW sample. MP degradation rate is impeded in relation to UPW by about 60% but still is faster than in WW. The effect of bicarbonate, the dominant anion in natural waters, is depicted in Fig. 5b. The addition of 250 mg/L bicarbonate in UPW (this concentration matches that in the BW sample) retards MP degradation by ca. 50%. A similarly negative effect is associated with the addition of chloride in UPW, as can be seen in Fig. 5c. It is documented that bicarbonate [33,34] can scavenge hydroxyl radicals to form carbonate radicals ($CO_3^{\cdot -}$), whose oxidation potential is 35% lower than hydroxyl radicals (Eq. (7)).

$$HCO_3^- + HO^{\cdot} \rightarrow CO_3^{\cdot -} + H_2O \quad (7)$$

On the other hand, chloride reacts with hydroxyl radicals (Eq. (8)) to form the less reactive chlorine radicals (Eq. (9)) [35], whose formation is favored in neutral to acidic condition (pH < 7.2) [36].

$$Cl^- + HO^{\cdot} \rightarrow HOCl^{\cdot -} \quad (8)$$

$$HOCl^{\cdot -} + H^+ \rightarrow Cl^{\cdot} + H_2O \quad (9)$$

The influence of solution pH on MP degradation is presented in Fig. 6. The inherent pH = 6 of UPW was adjusted to acidic or alkaline conditions adding a measured volume of acid or alkali, correspondingly. Degradation is favored at inherent pH but retarded at acidic or alkaline conditions. The p*K* value of MP is about 8.5, while the pzc value of CX/CoFe is 7.7 [18]. This means that at pH = 6, the surface of the CX/CoFe catalyst is slightly positive and MP is almost neutral, with only a small amount positively charged. On the contrary, at pH = 3 the surface of CX/CoFe and MP are highly positively charged and electrostatic repulsion occurs, thus reducing degradation. At pH = 10, part of hydroxyl radicals are neutralized reacting with hydroxyl anions to produce oxygen, while the highly negative charge of MP and the catalyst surface worsens the adsorption process.

It must be pointed out that the effect of pH may partly explain the effect of actual water matrices shown in Fig. 5a. For example, the slower MP degradation in WW may be associated, to some extent, with the basic pH (i.e. 8) of the matrix.

In general, sonochemical degradation reactions may occur in three regions, namely (i) the bubble itself, whereas pyrolytic reactions are likely to occur (ii) at the vicinity of the bubble–liquid interface, and (iii) in the liquid bulk; in the latter two cases, radical reactions are likely to dominate [15]. Experiments were conducted in UPW spiked with an excess of various organics that can deliberately interfere with MP degradation, in an attempt to identify the most probable reaction sites; the results are summarized in Fig. 7. *t*–Butanol, an effective hydroxyl radical scavenger in water sonolysis [37], quenches the reaction leading to only ca 20% of MP degradation after 60 min. The addition of either sodium dodecyl sulfate (SDS) or sodium acetate, both having surfactant properties, is also detrimental to degradation; surfactants comprising hydrophilic and hydrophobic parts are likely to position themselves in the bubble–liquid interface, thus restricting reactions at this site. The presence of glucose, which is expected to compete for the reactive species in the liquid bulk since it is fully soluble, also retards degradation. In this view, radical reactions in the vicinity of the interface and in the liquid bulk seem to be responsible for the sonochemical degradation of MP.

All the experiments described so far were conducted under air–equilibrated conditions. To verify the role of hydroxyl radical and other oxygen species, additional experiments were performed under a continuous flow of nitrogen and the results are depicted in Fig. 8. As clearly seen, stripping of oxygen from the liquid phase is detrimental to MP degradation both in the presence and absence of catalyst. In addition to the reactions (3)–(5), which are directly related to water sonolysis, the presence of oxygen can trigger the reactions (10)–(13), thus enhancing the formation of hydroxyl and hydroperoxyl radicals [15,38]:

$$O2 \overset{)))}{\rightarrow} 2O \quad (10)$$

$$H_2O_2 + O \rightarrow HOO^{\cdot} + HO^{\cdot} \quad (11)$$

$$O_2 + H^{\cdot} \rightarrow HOO^{\cdot} \quad (12)$$

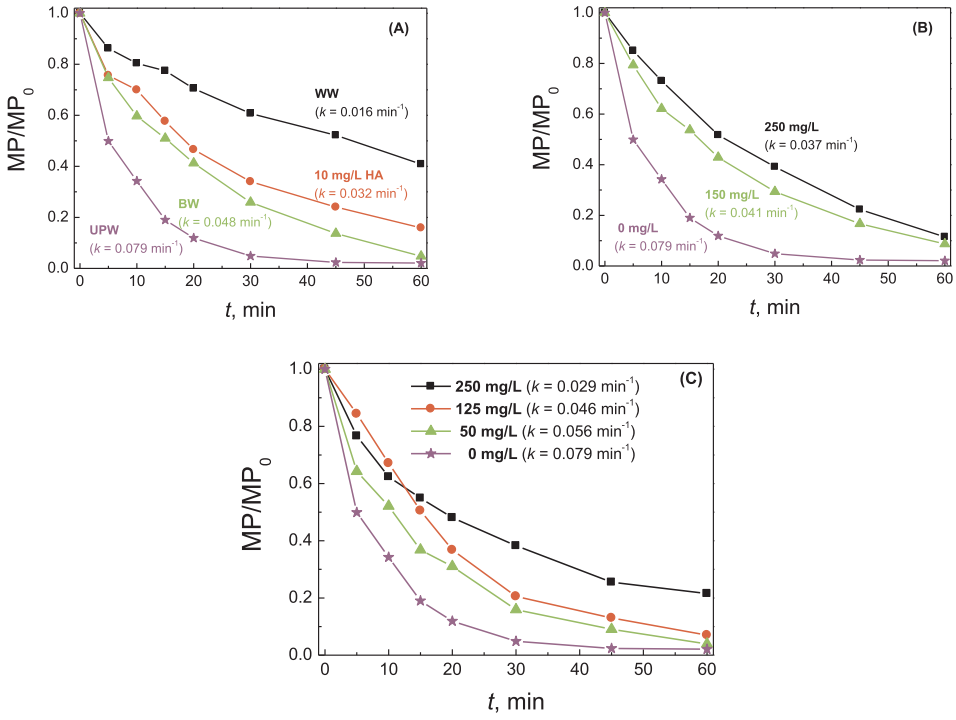

Fig. 5. Effect of water constituents on 1 mg/L MP sonocatalytic degradation at 52 W/L with 25 mg/L CX/CoFe. (A) Actual matrices and UPW spiked with HA; (B) UPW spiked with bicarbonate at various concentrations; (C) UPW spiked with chloride at various concentrations. Numbers in brackets show k values in min^{-1}.

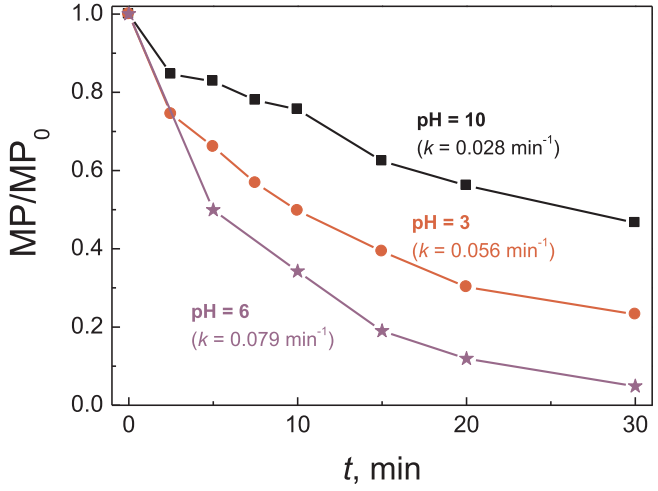

Fig. 6. Effect of the initial solution pH on 1 mg/L MP sonocatalytic degradation at 52 W/L with 25 mg/L CX/CoFe in UPW. Numbers in brackets show k values in min^{-1}.

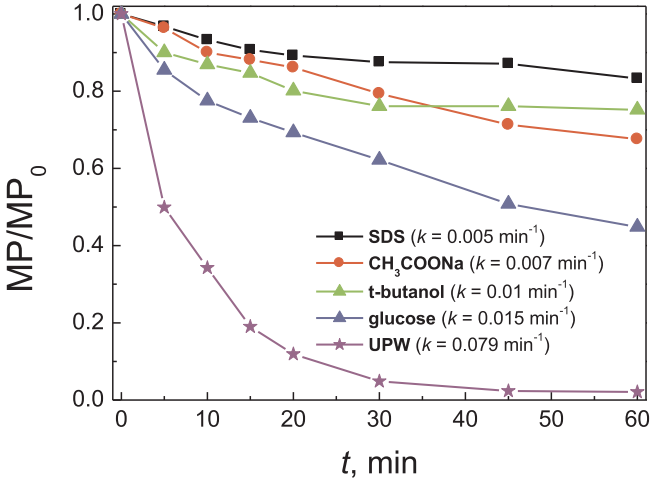

Fig. 7. Effect of various scavengers on 1 mg/L MP sonocatalytic degradation at 52 W/L with 25 mg/L CX/CoFe in UPW. Numbers in brackets show k values in min^{-1}. All scavengers were added at 2 g/L except butanol at 10 g/L.

$$HOO^{\cdot} + HOO^{\cdot} \rightarrow H_2O_2 + O_2 \quad (13)$$

The absence of the reactions (10)–(13) under nitrogen sparging presumably suppresses the formation of reactive oxygen species and, consequently, MP degradation. It should be mentioned here that water saturated with nitrogen may improve the formation of other reactive species such as nitrate and nitrite radicals [38,39]; however, this seems inadequate to compensate for the loss of oxygen species in the system.

Catalyst stability, which is considered a basic requirement for real scale applications, was also studied. A series of four sonocatalytic runs was performed with consecutive reuse of CX/CoFe. The in-situ magnetic separation procedure previously reported for the recovery of CX/CoFe after the treatment stage was employed for that purpose [18]. Briefly, the catalyst was separated after each run by allowing its deposition on the magnetic stirring bar. Afterwards, the treated water was recovered, and the catalyst was reused upon the addition of a fresh MP solution. As seen in Fig. 9, MP degradation obtained after 45 min is not particularly affected by the successive reuse of the catalyst, thus revealing the high stability of CX/CoFe for the sonocatalytic treatment process, and its potential usefulness for practical applications. Nevertheless, a slight decrease in the degradation kinetics is observed from the 1st to the 2nd cycle, which may be due to an increased contribution of pure adsorption in the early stage of the 1st cycle. Afterwards, from the 2nd to the 4th cycle, the kinetics of MP degradation remain unaffected.

4. Conclusions

The following conclusions can be drawn from this study:

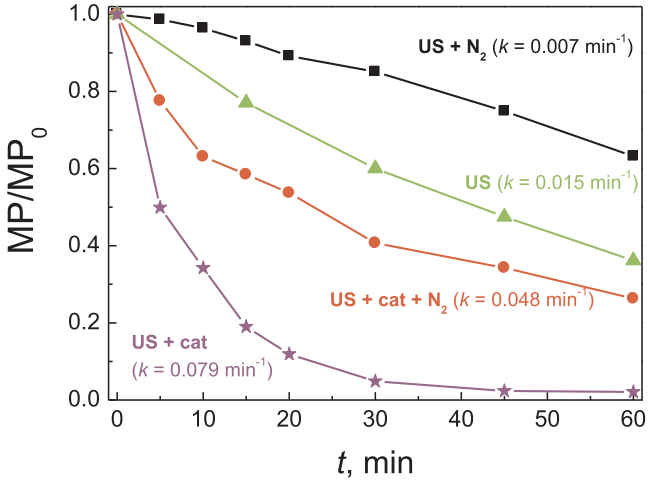

Fig. 8. Effect of nitrogen sparging on 1 mg/L MP degradation at 52 W/L with and without 25 mg/L CX/CoFe in UPW. Numbers in brackets show k values in min^{-1}.

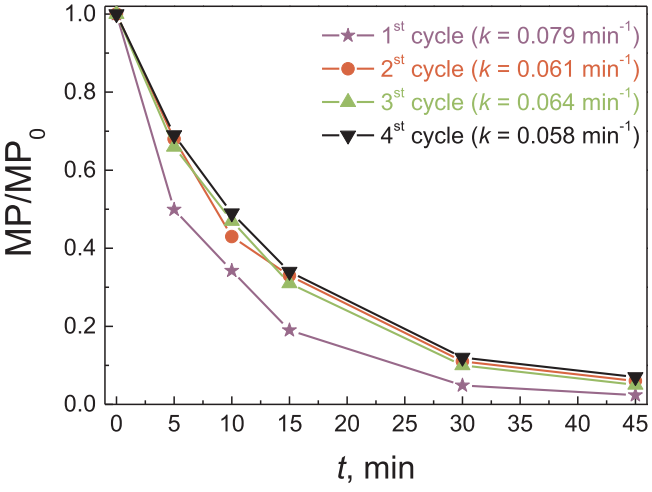

Fig. 9. Degradation of 1 mg/L MP in UPW. obtained in a series of four sonocatalytic runs performed with consecutive reuse of CX/CoFe (25 mg/L) at 52 W/L. Numbers in brackets show k values in min^{-1}.

1) Methylparaben can be degraded by low frequency ultrasound and the rate increases with increasing power density. The presence of a carbon xerogel containing cobalt and iron enhances degradation in a synergistic way. This is, to a certain degree, due to CX/CoFe catalyzing the dissociation of hydrogen peroxide, formed through water sonolysis, to hydroxyl radicals.
2) Sonocatalytic degradation mainly occurs through reactions involving hydroxyl radicals and other oxygen species that occur in the vicinity of the bubble–liquid interface and in the bulk solution. This is evidenced through experiments (i) adding conventional radical scavengers and surfactants, and (ii) purging oxygen from the reaction mixture.
3) Water matrix effects are detrimental to sonocatalytic degradation of methylparaben. This seems to be due to various inorganic and organic species inherently present in natural waters and wastewaters.
4) The addition of persulfate salt as an extra source of radicals activated by both the ultrasound and the catalyst is inhibitory to the sonocatalytic reaction. It may be hypothesized that an excessive amount of radicals generated by the combined process leads to self–scavenging reactions.
5) CX/CoFe revealed high stability for the sonocatalytic degradation of methylparaben, as shown by performing a series of four cycles with consecutive catalyst reuse.

Declaration of Competing Interest

The authors declare that they have no known competing financial interests or personal relationships that could have appeared to influence the work reported in this paper.

Acknowledgements

This work is a result of: project “AIProcMat@N2020 - Advanced Industrial Processes and Materials for a Sustainable Northern Region of Portugal 2020”, with the reference NORTE-01-0145-FEDER-000006, supported by Norte Portugal Regional Operational Programme (NORTE2020), under the Portugal 2020 Partnership Agreement, through the European Regional Development Fund (ERDF); Project Associate Laboratory LSRE-LCM – UID/EQU/50020/2019 – funded by national funds through FCT/MCTES (PIDDAC).

Appendix A. Supplementary data

Supplementary data to this article can be found online at https://doi.org/10.1016/j.ultsonch.2020.105045.

References

[1] C. Haman, X. Dauchy, C. Rosin, J.-F. Munoz, Occurrence, fate and behavior of parabens in aquatic environments: a review, Water Res. 68 (2015) 1–11, https://doi.org/10.1016/j.watres.2014.09.030.
[2] J. Xue, K. Kannan, Accumulation profiles of parabens and their metabolites in fish, black bear, and birds, including bald eagles and albatrosses, Environ. Int. 94 (2016) 546–553, https://doi.org/10.1016/j.envint.2016.06.015.
[3] P.D. Darbre, A. Aljarrah, W.R. Miller, N.G. Coldham, M.J. Sauer, G.S. Pope, Concentrations of parabens in human breast tumours, J. Appl. Toxicol. 24 (2004) 5–13, https://doi.org/10.1002/jat.958.
[4] J.-W. Lee, H.-K. Lee, H.-B. Moon, Contamination and spatial distribution of parabens, their metabolites and antimicrobials in sediment from Korean coastal waters, Ecotoxicol. Environ. Safe. 180 (2019) 185–191, https://doi.org/10.1016/j.ecoenv.2019.05.012.
[5] D. Molins-Delgado, M.S. Díaz-Cruz, D. Barceló, Ecological risk assessment associated to the removal of endocrine-disrupting parabens and benzophenone-4 in wastewater treatment, J. Hazard. Mater. 310 (2016) 143–151, https://doi.org/10.1016/j.jhazmat.2016.02.030.
[6] T. Velegraki, E. Hapeshi, D. Fatta-Kassinos, I. Poulios, Solar–induced heterogeneous photocatalytic degradation of methyl–paraben, Appl. Catal. B 178 (2015) 2–11, https://doi.org/10.1016/j.apcatb.2014.11.022.
[7] X. Feng, Y. Chen, Y. Fang, X. Wang, Z. Wang, T. Tao, Y. Zuo, Photodegradation of parabens by Fe(III)–citrate complexes at circumneutral pH: Matrix effect and reaction mechanism, Sci. Total Environ. 472 (2014) 130–136, https://doi.org/10.1016/j.scitotenv.2013.11.005.
[8] M. Gmurek, A.F. Rossi, R.C. Martins, R.M. Quinta-Ferreira, S. Ledakowicz, Photodegradation of single and mixture of parabens – Kinetic, by–products identification and cost–efficiency analysis, Chem. Eng. J. 276 (2015) 303–314, https://doi.org/10.1016/j.cej.2015.04.093.
[9] Z. Frontistis, M. Antonopoulou, A. Petala, D. Venieri, I. Konstantinou, D.I. Kondarides, D. Mantzavinos, Photodegradation of ethyl paraben using simulated solar radiation and Ag_3PO_4 photocatalyst, J. Hazard. Mater. 323 (2017) 478–488, https://doi.org/10.1016/j.jhazmat.2016.04.017.
[10] S. Dhaka, R. Kumar, M.A. Khan, K.-J. Paeng, M.B. Kurade, S.-J. Kim, B.-H. Jeon, Aqueous phase degradation of methyl paraben using UV–activated persulfate method, Chem. Eng. J. 321 (2017) 11–19, https://doi.org/10.1016/j.cej.2017.03.085.
[11] Y. Chen, P. Deng, P. Xie, R. Shang, Z. Wang, S. Wang, Heat–activated persulfate oxidation of methyl– and ethyl–parabens: Effect, kinetics, and mechanism, Chemosphere 168 (2017) 1628–1636, https://doi.org/10.1016/j.chemosphere.2016.11.143.
[12] D. Dionisio, A.J. Motheo, C. Sáez, M.A. Rodrigo, Effect of the electrolyte on the electrolysis and photoelectrolysis of synthetic methyl paraben polluted wastewater, Sep. Purif. Technol. 208 (2019) 201–207, https://doi.org/10.1016/j.seppur.2018.03.009.
[13] S. Sasi, M.P. Rayaroth, D. Devadasan, U.K. Aravind, C.T. Aravindakumar, Influence of inorganic ions and selected emerging contaminants on the degradation of methylparaben: A sonochemical approach, J. Hazard. Mater. 300 (2015) 202–209, https://doi.org/10.1016/j.jhazmat.2015.06.072.
[14] C. Papadopoulos, Z. Frontistis, M. Antonopoulou, D. Venieri, I. Konstantinou, D. Mantzavinos, Sonochemical degradation of ethyl paraben in environmental samples: Statistically important parameters determining kinetics, by–products and pathways, Ultrason. Sonochem. 31 (2016) 62–70, https://doi.org/10.1016/j.

ultsonch.2015.12.002.
[15] N. Ince, G. Tezcanli, R. Belen, İ. Apikyan, Ultrasound as a catalyzer of aqueous reaction systems: the state of the art and environmental applications, Appl. Catal. B 29 (2001) 167–176, https://doi.org/10.1016/S0926-3373(00)00224-1.
[16] B. Savun-Hekimoğlu, N.H. Ince, Sonochemical and sonocatalytic destruction of methylparaben using raw, modified and SDS-intercalated particles of a natural clay mineral, Ultrason. Sonochem. 54 (2019) 233–240, https://doi.org/10.1016/j.ultsonch.2019.01.034.
[17] G. Bampos, Z. Frontistis, Sonocatalytic degradation of butylparaben in aqueous phase over Pd/C nanoparticles, Environ. Sci. Poll. Res. 26 (2019) 11905–11919, https://doi.org/10.1007/s11356-019-04604-5.
[18] R.S. Ribeiro, Z. Frontistis, D. Mantzavinos, D. Venieri, M. Antonopoulou, I. Konstantinou, A.M.T. Silva, J.L. Faria, H.T. Gomes, Magnetic carbon xerogels for the catalytic wet peroxide oxidation of sulfamethoxazole in environmentally relevant water matrices, Appl. Catal. B 199 (2016) 170–186, https://doi.org/10.1016/j.apcatb.2016.06.021.
[19] R.S. Ribeiro, A.M.T. Silva, J.L. Figueiredo, J.L. Faria, H.T. Gomes, The role of cobalt in bimetallic iron-cobalt magnetic carbon xerogels developed for catalytic wet peroxide oxidation, Catal. Today 296 (2017) 66–75, https://doi.org/10.1016/j.cattod.2017.06.023.
[20] A. Outsiou, Z. Frontistis, R.S. Ribeiro, M. Antonopoulou, I. Konstantinou, A.M.T. Silva, J.L. Faria, H.T. Gomes, D. Mantzavinos, Activation of sodium persulfate by magnetic carbon xerogels (CX/CoFe) for the oxidation of bisphenol A: Process variables effects, matrix effects and reaction pathways, Water Res. 124 (2017) 97–107, https://doi.org/10.1016/j.watres.2017.07.046.
[21] M.E. Metheniti, Z. Frontistis, R.S. Ribeiro, A.M.T. Silva, J.L. Faria, H.T. Gomes, D. Mantzavinos, Degradation of propyl paraben by activated persulfate using iron–containing magnetic carbon xerogels: Investigation of water matrix and process synergy effects, Environ. Sci. Poll. Res. 25 (2018) 34801–34810, https://doi.org/10.1007/s11356-017-0178-9.
[22] R.S. Ribeiro, A.M.T. Silva, J.L. Figueiredo, J.L. Faria, H.T. Gomes, Catalytic wet peroxide oxidation: a route towards the application of hybrid magnetic carbon nanocomposites for the degradation of organic pollutants, A review, Appl. Catal. B 187 (2016) 428–460, https://doi.org/10.1016/j.apcatb.2016.01.033.
[23] Y. Wang, H. Zhao, G. Zhao, Iron-copper bimetallic nanoparticles embedded within ordered mesoporous carbon as effective and stable heterogeneous Fenton catalyst for the degradation of organic contaminants, Appl. Catal. B 164 (2015) 396–406, https://doi.org/10.1016/j.apcatb.2014.09.047.
[24] R.F.P. Nogueira, M.C. Oliveira, W.C. Paterlini, Simple and fast spectrophotometric determination of H_2O_2 in photo-Fenton reactions using metavanadate, Talanta 66 (2005) 86–91, https://doi.org/10.1016/j.talanta.2004.10.001.
[25] Z. Frontistis, D. Mantzavinos, Advanced oxidation processes for wastewater treatment, in: I.K. Kalavrouziotis (Ed.), Wastewater and biosolids management, first ed., IWA Publishing, London, 2017, pp. 131–143.
[26] K. Makino, M.M. Mossoba, P. Riesz, Chemical effects of ultrasound on aqueous solutions. Formation of hydroxyl radicals and hydrogen atoms, J. Phys. Chem. 87 (1983) 1369–1377, https://doi.org/10.1021/j100231a020.
[27] M. Gutierrez, A. Henglein, J.K. Dohrmann, Hydrogen atom reactions in the sonolysis of aqueous solutions, J. Phys. Chem. 91 (1987) 6687–6690, https://doi.org/10.1021/j100311a026.
[28] G. Fang, X. Chen, W. Wu, C. Liu, D.D. Dionysiou, T. Fan, Y. Wang, C. Zhu, D. Zhou, Mechanisms of interaction between persulfate and soil constituents: Activation, free radical formation, conversion, and identification, Environ. Sci. Technol. 52 (2018) 14352–14361, https://doi.org/10.1021/acs.est.8b04766.
[29] E. Magioglou, Z. Frontistis, J. Vakros, I.D. Manariotis, D. Mantzavinos, Activation of persulfate by biochars from valorized olive stones for the degradation of sulfamethoxazole, Catalysts 9 (2019) 419–432, https://doi.org/10.3390/catal9050419.
[30] G.P. Anipsitakis, D.D. Dionysiou, Radical generation by the interaction of transition metals with common oxidants, Environ. Sci. Technol. 38 (2004) 3705–3712, https://doi.org/10.1021/es035121o.
[31] L. Kemmou, Z. Frontistis, J. Vakros, I.D. Manariotis, D. Mantzavinos, Degradation of antibiotic sulfamethoxazole by biochar–activated persulfate: Factors affecting the activation and degradation processes, Catal. Today 313 (2018) 128–133, https://doi.org/10.1016/j.cattod.2017.12.028.
[32] L.W. Matzek, K.E. Carter, Activated persulfate for organic chemical degradation: A review, Chemosphere 151 (2016) 178–188, https://doi.org/10.1016/j.chemosphere.2016.02.055.
[33] C. Petrier, R. Torres-Palma, E. Combet, G. Sarantakos, S. Baup, C. Pulgarin, Enhanced sonochemical degradation of bisphenol–A by bicarbonate ions, Ultrason. Sonochem. 17 (2010) 111–115, https://doi.org/10.1016/j.ultsonch.2009.05.010.
[34] M. Chiha, O. Hamdaoui, S. Baup, N. Gondrexon, Sonolytic degradation of endocrine disrupting chemical 4–cumylphenol in water, Ultrason. Sonochem. 18 (2011) 943–950, https://doi.org/10.1016/j.ultsonch.2010.12.014.
[35] D.A. Armstrong, R.E. Huie, S. Lymar, W.H. Koppenol, G. Merényi, P. Neta, D.M. Stanbury, S. Steenken, P. Wardman, Standard electrode potentials involving radicals in aqueous solution: inorganic radicals, Bioinorg. React. Mech. 9 (2013) 59–61, https://doi.org/10.1515/irm-2013-0005.
[36] C.-H. Liao, S.-F. Kang, F.-A. Wu, Hydroxyl radical scavenging role of chloride and bicarbonate ions in the H_2O_2/UV process, Chemosphere 44 (2001) 1193–1200, https://doi.org/10.1016/S0045-6535(00)00278-2.
[37] H. Okuno, B. Yim, Y. Mizukoshi, Y. Nagata, Y. Maeda, Sonolytic degradation of hazardous organic compounds in aqueous solution, Ultrason. Sonochem. 7 (2000) 261–264, https://doi.org/10.1016/S1350-4177(00)00053-5.
[38] Y.G. Adewuyi, Sonochemistry: Environmental science and engineering applications, Ind. Eng. Chem. Res. 40 (2001) 4681, https://doi.org/10.1021/ie010096l.
[39] I. Gultekin, N.H. Ince, Ultrasonic destruction of bisphenol-A: The operating parameters, Ultrason. Sonochem. 15 (2008) 524–529, https://doi.org/10.1016/j.ultsonch.2007.05.005.